TECHNICAL REPORTS

nature medicine

Tracking metastatic tumor cell extravasation with quantum dot nanocrystals and fluorescence emission-scanning microscopy

Evelyn B Voura[1], Jyoti K Jaiswal[1], Hedi Mattoussi[2] & Sanford M Simon[1]

Metastasis is an impediment to the development of effective cancer therapies. Our understanding of metastasis is limited by our inability to follow this process *in vivo*. Fluorescence microscopy offers the potential to follow cells at high resolution in living animals. Semiconductor nanocrystals, quantum dots (QDs), offer considerable advantages over organic fluorophores for this purpose. We used QDs and emission spectrum scanning multiphoton microscopy to develop a means to study extravasation *in vivo*. Although QD labeling shows no deleterious effects on cultured cells, concern over their potential toxicity *in vivo* has caused resistance toward their application to such studies. To test if effects of QD labeling emerge *in vivo*, tumor cells labeled with QDs were intravenously injected into mice and followed as they extravasated into lung tissue. The behavior of QD-labeled tumor cells *in vivo* was indistinguishable from that of unlabeled cells. QDs and spectral imaging allowed the simultaneous identification of five different populations of cells using multiphoton laser excitation. Besides establishing the safety of QDs for *in vivo* studies, our approach permits the study of multicellular interactions *in vivo*.

Most information regarding the critical stages of metastasis has traditionally been gathered using culture-based assays or *in vivo* models. These approaches have generated several hypotheses describing the nature of the processes and have suggested possible therapeutic targets[1–3]. Yet the process of extravasation remains poorly understood. Our knowledge is limited by the inaccessibility of the phenomena to the experimental tools necessary to visualize the multicellular and multimolecular interactions taking place deep within tissues. Although *in vitro* assays provide details of molecular interactions during experimental conditions, they lack the complexity of the physiological environment found in whole-animal studies[4–6]. Conversely, whole-animal studies have relied on tumor endpoint analyses. This necessitates inferring cellular interactions during tumor cell extravasation from changes in final tumor counts[7,8], making it difficult to test hypotheses and thus limiting our understanding of the process. Difficulties rendered by either method of investigation likely result in hypotheses contributing to disappointing clinical trials, as exemplified by those targeting proteolysis[9].

In vivo microscopy[10,11] avoids the problems of endpoint analysis. The resolution with fluorescent multiphoton *in vivo* microscopy can reach the single-cell level[12,13]. Such imaging has used two groups of organic fluorophores: the fluorescent proteins expressed by the cells themselves and fluorescent dyes that are exogenously loaded into the cells[14]. Organic fluorophores have numerous limitations restricting their usefulness for *in vivo* imaging. One is the difficulty in simultaneously imaging multiple independent organic fluorophores. This limitation is based on two characteristics of these fluorophores. First, they require distinct excitation wavelengths and have a very small Stokes shift between excitation and emission wavelengths. Thus, multiple excitation lines are needed for imaging multiple fluorophores and each additional excitation line limits the spectra available for emission collection. Second, they emit over a broad region of the visible spectra. Thus the emissions of different fluorophores overlap with each other and with much of the tissue autofluorescence. A second limitation of organic fluorophores is their susceptibility to photodamage and metabolic degradation, which restricts their use in long-term *in vivo* imaging. Moreover, some organic fluorophores, such as fluorescein, have a limited response to multiphoton excitation, which is a particular liability when trying to image into tissues.

In contrast, the fluorescent inorganic nanocrystals called QDs lack these limitations[15]. They can be excited by a wide spectrum of single and multiphoton excitation light, which is well separated from their emission spectra[16–18]. Thus, only one excitation wavelength is needed to simultaneously excite several different QDs. QDs also have narrow emission spectra, which are tunable to any desired wavelength from blue to infrared[19–22]. Thus from their emission spectra several different QDs can be easily distinguished from each other. QDs are also virtually resistant to photobleaching and are as bright as the best-known organic fluorophores[17,18,23]. Further, they have a good multiphoton absorption between 700 and 1,000 nm[18–21].

These features make QDs desirable for long-term multicolor *in vivo* imaging[23]. However, concern over the potential toxicity of the metals

[1]The Rockefeller University, Box 304, 1230 York Avenue, New York, New York, USA. [2]Division of Optical Sciences, US Naval Research Laboratory, 4555 Overlook Avenue SW, Washington, DC, USA. Correspondence should be addressed to S.M.S. (simon@rockefeller.edu).

Published online 29 August 2004; doi:10.1038/nm1096

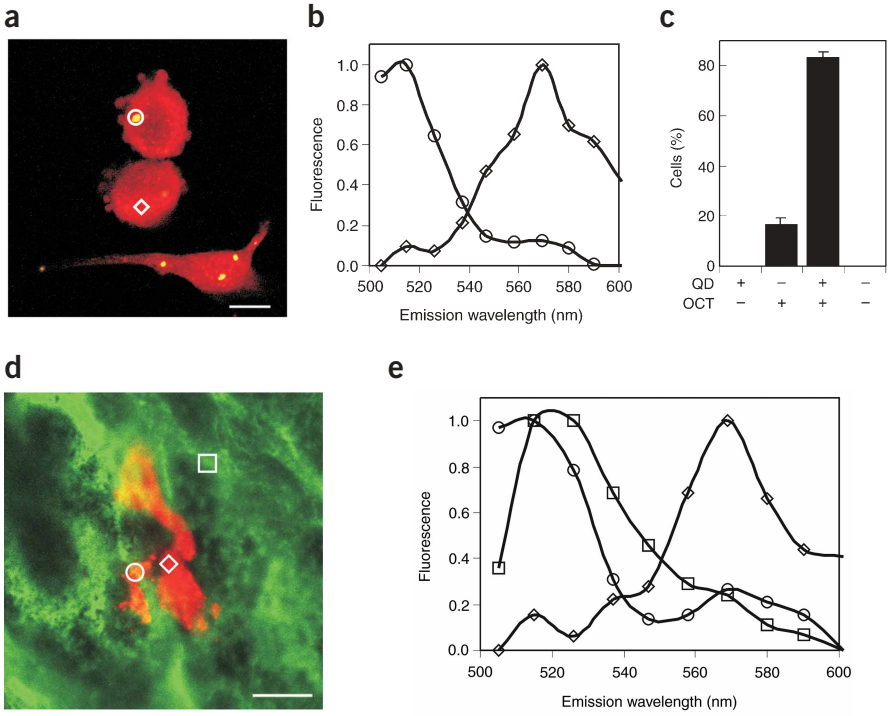

Figure 1 Intracellular labeling of tumor cells by QDs permits *in vivo* imaging despite tissue autofluorescence. (**a**) Use of DNA transfection reagent Lipofectamine 2000 allowed the orange cell tracker-labeled B16F10 tumor cells to be tagged with DHLA-capped, 510-nm QDs (yellow). (**b**) Emission-scanning confocal microscopy using META detector with cells dual-labeled with QDs (circles) and orange cell tracker (diamonds) allowed identifying them based on their emission spectra (excitation 488 nm). (**c**) Use of Lipofectamine 2000 allowed labeling of >80% of the B16F10 tumor cells. (**d**) B16F10 cells labeled with 510-nm QD (yellow) and orange cell tracker (OCT; red) were injected into the tail vein of mouse. At 5 h after injection lung tissue was fixed in formalin as whole mounts and labeled with fluorescein lycopersicon esculentum lectin (green) to mark the endothelial cells. A three-dimensional projection of a whole-mount lung tissue made using 1-μm optical sections. (**e**) The emission scans for 510-nm QD (circles), orange cell tracker (diamonds) and lectin (squares). Scale bars, 10 μm. The error bars represent standard error. Fluorescence measurements are given in arbitrary units.

used in the core of QDs, such as cadmium-selenium, has limited their application for *in vivo* imaging. We show that tumor cells labeled with QDs survived the selective pressure of the circulation and managed to extravasate into tissues just as effectively as unlabeled cells. QDs had no detectable adverse effects on the physiology of the host animal or the QD-labeled cells, even when subjected to selective pressures of tumor growth for extended periods. Further, we demonstrate the utility of emission scanning one- and two-photon microscopy and QDs for simultaneous imaging of *in vivo* interactions of multiple populations of QD-labeled tumor cells, with each other and with the rest of the tissue.

RESULTS

Our goal was to establish a model to follow tumor cell extravasation in a living animal. The approach was to use tumor cells labeled with QDs. We chose a well-established model of cancer cell metastasis, based on the injection of B16 melanoma cells into syngeneic C57BL/6 mice[24,25].

In previous studies we used endocytosis and cell-surface biotinylation to label cells with QDs[23]. Biotinylation, however, might alter cell surface proteins, affecting cellular interactions and, ultimately, migration of invading tumor cells. Although endocytic labeling is not deleterious to cells, it requires the use of large amounts of QDs. Thus, to label cells with QDs we needed an approach that required fewer QDs and did not alter the cell surface.

Intracellular labeling of tumor cells by QDs

Our dihydroxylipoic acid (DHLA)-capped QDs are negatively charged[16]. Because cationic lipids can efficiently transduce negatively charged nucleic acids into the cytoplasm[26] and are considered safe and reliable for therapeutic gene delivery[27], we tested whether cationic lipids could load DHLA-capped QDs into tumor cells. Using Lipofectamine 2000, QDs were efficiently delivered into cells (**Fig. 1a**, 510-nm emission). Inside cells, QDs retained their spectral profile and were distinguished from other fluorophores (**Fig. 1b**). With this technique, 85–95% of the cells were consistently loaded with QDs (**Fig. 1c**). Even after 14 d of growth, no detectable difference in the growth of QD-labeled and unlabeled cells was observed (data not shown). Cationic lipid-based loading of QDs resulted in the formation of intracellular QD aggregates of varied fluorescence intensity (**Fig. 1a**). As these aggregates formed during the incubation with cationic lipids, they may result from the same lipid-based processes that aggregate nucleic acids[26].

In vivo imaging of QD-labeled cells

We injected the tail veins of C57BL/6 mice with $2–4 \times 10^5$ B16F10 cells labeled with orange cell tracker dye (Molecular Probes cell tracker CMTMR) and QDs. After 5 h, the mice were killed and the lungs extracted, fixed in formalin and labeled with fluorescein lycopersicum esculentin lectin. Whole mounts were examined using emission-scanning microscopy with a 10-nm bandwidth from each pixel in the image using a Zeiss META detector. This allowed us to distinguish the emission from QDs (circles), orange cell tracker (diamonds) and lectin (squares) from each other and from the tissue autofluorescence[28] (**Fig. 1d,e** and **Supplementary Fig. 1** online). Because the region around the QDs is also labeled with the orange cell tracker, the resulting emission spectra show two peaks. Furthermore, the 10-nm bandwidth used by the META detector can slightly shift the apparent peak emission of the 510-nm QD to range between 505 nm and 515 nm.

After injection into the tail vein, tumor cells labeled with orange cell tracker and 510-nm QDs were detectable in the lung (**Fig. 1d,e**). It has been proposed that most tumor cells do not survive the rigors of the circulation[2]. Thus we were concerned that dying cells might release QDs into the bloodstream. If released QDs were not rapidly cleared from the circulation, they might lodge in the lung tissues or be ingested by phagocytic cells in the lungs, thus giving us false-positive results. If QDs are released by dying tumor cells and then phagocytosed by immune cells, the resulting QD-labeled immune cells would

not simultaneously show cytosolic labeling with the cell tracker dye. In lung tissues collected 30 min to 5 h after injection, we did not detect 510-nm QD-labeled cells that were not colabeled with orange cell tracker dye. The experiment was repeated using 570-nm and 610-nm QDs and blue cell tracker dye. Again, we did not find evidence of cells that were labeled with QDs but not with the cell tracker dye. This indicates that QDs were present only in the injected tumor cells and not in the cells of the host animal.

Tissues from other organs including liver (**Fig. 2a**,**b**) and spleen (**Fig. 2c**,**d**) were examined for the presence of 510-nm QD-labeled tumor cells. The number of cells per field labeled with orange cell tracker and 510-nm QD was lower in the spleen and liver than in the lung tissues. Once again, in these experiments all detectable QDs were colocalized with orange cell tracker. Thus, if QD-labeled tumor cells die in the circulation, QDs released by them must be efficiently cleared from the blood. This is in agreement with a recent report that showed most QDs were rapidly cleared from the circulation after intravenous injection, whereas some QDs accumulated in the liver, lymph nodes and bone marrow[29]. Unlike injecting QDs, we found no free QDs in the liver or spleen after injection of QD-labeled cells, indicating that QDs released by dying cells will not restrict the ability to track QD-labeled cells in these organs. The presence of QD-labeled tumor cells in other tissues indicates that not all the cells are trapped in the lung. A population of tumor cells is able to circumnavigate the lung capillary network and seed other organs, but these cells do not regularly form tumors in these organs. It remains to be determined in which other organs the tumor cells can seed but fail to form tumors.

QDs were observed in tissue sections despite aldehyde fixation (formalin and paraformaldehyde) and subsequent processing (**Fig. 2e**,**f** and **Supplementary Fig. 2** online). These treatments did not affect the intensity or peak of the QD emission spectra (**Supplementary Fig. 2** online). In the 5- to 10-μm-thick histological sections, the percentage of cells double-labeled with cell tracker dye and QDs was lower (data not shown). This is probably a result of the thin sections, which catch only a fragment of a cell because cationic lipid-based loading does not disperse QDs evenly throughout the cytoplasm. The clustering of QDs in the cytoplasm also precluded using QDs to study cellular morphological features such as the elongated and contorted shapes of the tumor cells trapped in the lung tissue (**Fig. 1**). Thus, when documentation of such features is necessary, dyes such as cell trackers could be used.

QDs are inert tags for *in vivo* studies

QDs have a core of crystalline cadmium and selenium, which may have adverse effects on cell viability[30]. Previously, we observed that labeling with QDs had no detectable effect on the survival and growth of HeLa cells or on the signaling, chemotaxis, differentiation and development of the amoeba *Dictyostelium discoideum*[23]. To use QDs for labeling and monitoring cells in live animals, however, it is necessary to determine whether QDs pose any deleterious effect on cell viability *in vivo*.

To test whether QDs affected the physiology of mammalian cells *in vivo*, we put QD-labeled cells under a strong selective pressure in which they had to compete against cells not labeled with QDs. The tumor-forming capacity of B16F10 tumor cells is well established and thus provides an ideal tool to ascertain whether QD labeling compromises the ability of tumor cells to seed and form tumors in the lungs after intravenous injection. After injecting mice with tumor cells of which only a subset have QDs, if the QDs adversely affected the ability of cells to survive in the circulation, bind to the endothelial cells or extravasate and invade target tissues, then the fraction of QD-labeled tumor cells in the tissue should be lower than during injection. If QDs adversely affected the ability of cells to form tumors or survive attack by the immune system, then the fraction of nodules formed by QD-labeled tumor cells should be lower than the fraction of QD-labeled cells during injection.

Mice were injected with a population of tumor cells in which all of the cells were labeled with orange cell tracker and 69 ± 3.7% of those cells were labeled with 510-nm QDs (**Fig. 3a**). When tumor cells were imaged in the lung after 5 h, 74 ± 3.8% of the cells labeled with orange tracker were also labeled with 510-nm QD. These results indicate that labeling the tumor cells had no detectable effect ($P = 0.44$) on their

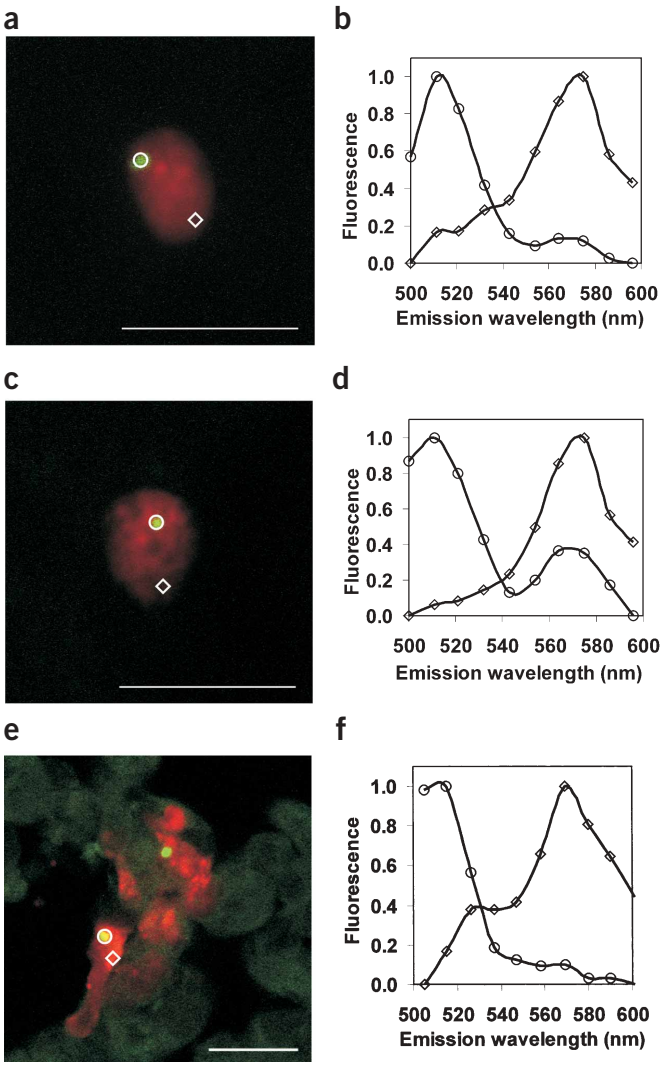

Figure 2 QDs can be used to study the distribution of tumor cells in organs and tissues. B16F10 cells labeled with 510-nm QD (yellow) and orange cell tracker (red) were injected into the tail vein of mouse and organs prepared as in **Figure 1d**. Representative images of 1-μm optical sections from liver (**a**) and spleen (**c**) and their corresponding emission scans (**b** and **d**, respectively) show the presence of labeled B16F10 cells in these organs. In another experiment, lung tissues from a mouse injected with 510-nm QD-labeled B16F10 cells were fixed in formalin, embedded in paraffin and sectioned (**e**). (**f**) Emission scan of **e**. All images were acquired using 488-nm laser excitation. Scale bars, 10 μm. Fluorescence measurements are given in arbitrary units.

ability to survive in the circulation or extravasate across the endothelium. To test whether QD labeling affects the ability of these cells to form tumors, mice were injected with QD-labeled tumor cells (>90% labeling) or an equal number of unlabeled tumor cells. When nodules were quantified in the mice after 40 d, there was no significant difference between the numbers of tumors formed in the two sets of mice (**Fig. 3b**; $P = 0.1$). Thus QD labeling of B16F10 cells does not affect their ability to form tumors.

QDs for multicolor imaging *in vivo*

QDs can be manufactured in a variety of emission wavelengths, each with relatively narrow emission spectra[19,22]. Use of emission spectrum scanning microscopy may enable simultaneously tracking several different QD-tagged populations of cells in the same animal[28]. To test this we loaded two populations of B16F10 cells with 510-nm or 570-nm QDs and plated them together. Mixing equal numbers of these cells did not result in cells being labeled with more than one color QD (**Fig. 4a,b**). This mixed population was injected into the tail vein, and lung tissues were extracted 5 h after injection, fixed in formalin and stained for actin for contrast (**Fig. 4c,d**). After excitation with 488-nm laser line, both populations of cells were identified in tissue whole mounts using emission-scanning microscopy. The number of QD-labeled B16F10 cells was quantified in 50 random fields. There was no statistical difference between the number of 510-nm and 570-nm QD-labeled cells (**Fig. 4e**; $P = 0.68$) in any of the fields. A correlation plot for the number of cells from these two populations in all of the fields indicates a strong correlation (correlation coefficient = 0.74) for colocalization of the two cell populations in the lungs (**Fig. 4f**). This suggests that the early seeding of the lung tissues by the B16F10 melanoma cells was not entirely a random process. More cells infiltrated certain locations while other areas had no tumor cells at all, suggesting that some areas of the lung are more conducive to extravasation than others.

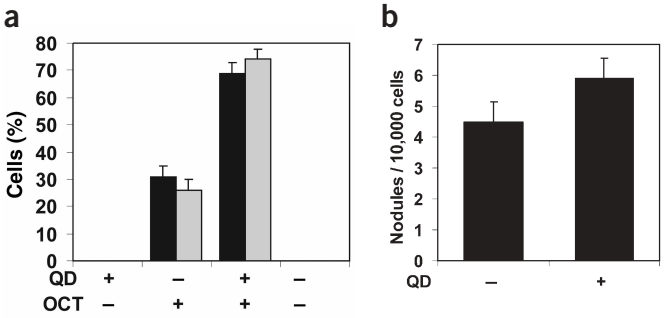

Figure 3 QD labeling has no effect on extravasation and tumor formation compared with unlabeled cells. 510-nm QD-labeled B16F10 cells (2×10^5) were either injected into the tail vein or cultured *in vitro*. (**a**) Labeling with QD and orange cell tracker of cells *in vitro* (black bars) was quantified on ten sets of ten random cells using epifluorescence microscopy. Labeled cells *in vivo* (gray bars) were counted in lung tissue prepared 5 h after injection as described in **Figure 1d**. No cells were found to be labeled with QDs alone. For tumor cells that extravasated into lungs, the relative number of cells labeled only with orange cell tracker (OCT) or colabeled with QDs remained the same as the cells in culture ($P = 0.44$). (**b**) To determine the tumor-forming potential of QD-labeled cells, two groups of mice were injected with tumor cells (2×10^5 each, either labeled or not labeled with QDs). Tumor nodules in lungs were counted in each mouse 40 d after injection. Both groups of mice had similar numbers of tumor nodules in their lungs ($P = 0.1$). The error bars represent standard error.

Multiphoton microscopy of QDs

As thicker tissues greatly absorb and scatter visible light, use of infrared excitation is highly desirable for *in vivo* imaging, a feature that has allowed the use of multiphoton microscopy for deep-tissue imaging. Because QDs are excellent multiphoton fluorescent probes with a broad excitation spectrum (700–1,000 nm), we carried out

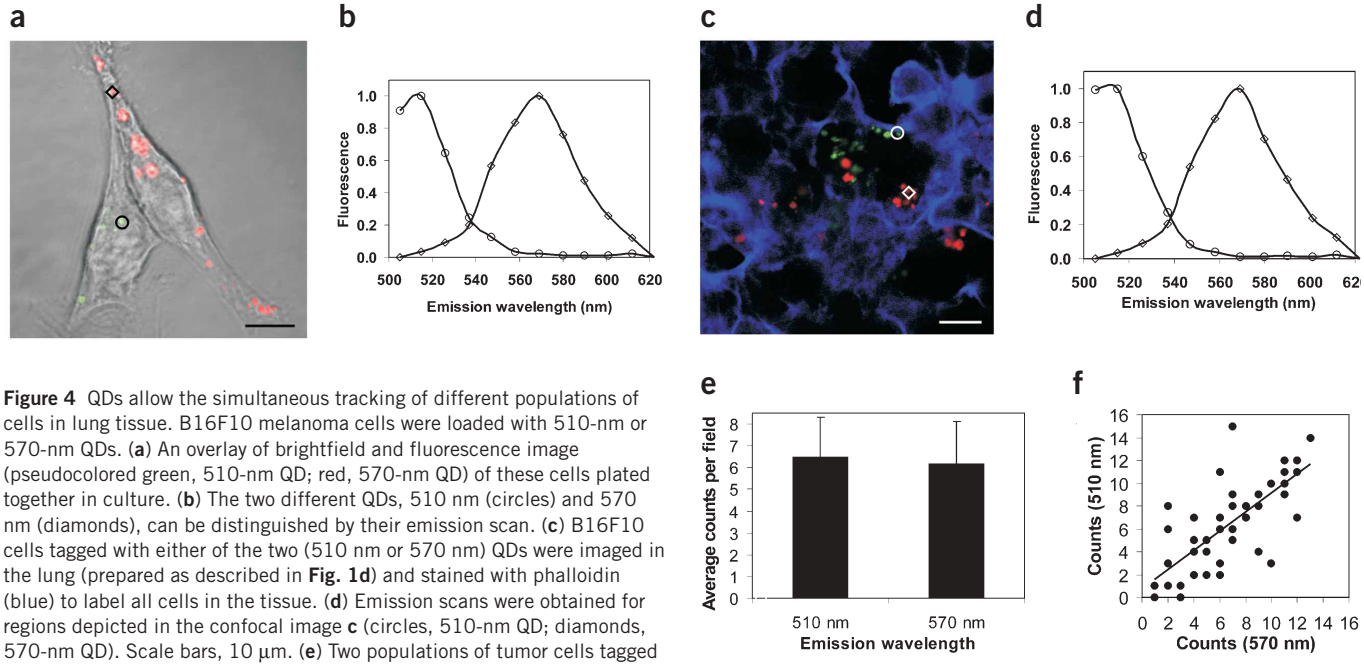

Figure 4 QDs allow the simultaneous tracking of different populations of cells in lung tissue. B16F10 melanoma cells were loaded with 510-nm or 570-nm QDs. (**a**) An overlay of brightfield and fluorescence image (pseudocolored green, 510-nm QD; red, 570-nm QD) of these cells plated together in culture. (**b**) The two different QDs, 510 nm (circles) and 570 nm (diamonds), can be distinguished by their emission scan. (**c**) B16F10 cells tagged with either of the two (510 nm or 570 nm) QDs were imaged in the lung (prepared as described in **Fig. 1d**) and stained with phalloidin (blue) to label all cells in the tissue. (**d**) Emission scans were obtained for regions depicted in the confocal image **c** (circles, 510-nm QD; diamonds, 570-nm QD). Scale bars, 10 μm. (**e**) Two populations of tumor cells tagged with 510-nm QD and 570-nm QD can be detected simultaneously in lung tissue using emission-scanning microscopy. Both populations of tumor cells extravasated equally well in lung tissue ($P = 0.68$), indicating no effect of the choice of QD on tumor cell extravasation. (**f**) The correlation plot for a representative experiment indicates that the number of 510-nm QD-labeled tumor cells is correlated with the number of 570-nm QD-labeled tumor cells (correlation coefficient = 0.74; R^2 value for the best fit line = 0.553). Total events in 50 fields were 323 for 510-nm QD-labeled cells and 309 for 570-nm QD-labeled cells. The error bars represent standard error. Fluorescence measurements are given in arbitrary units.

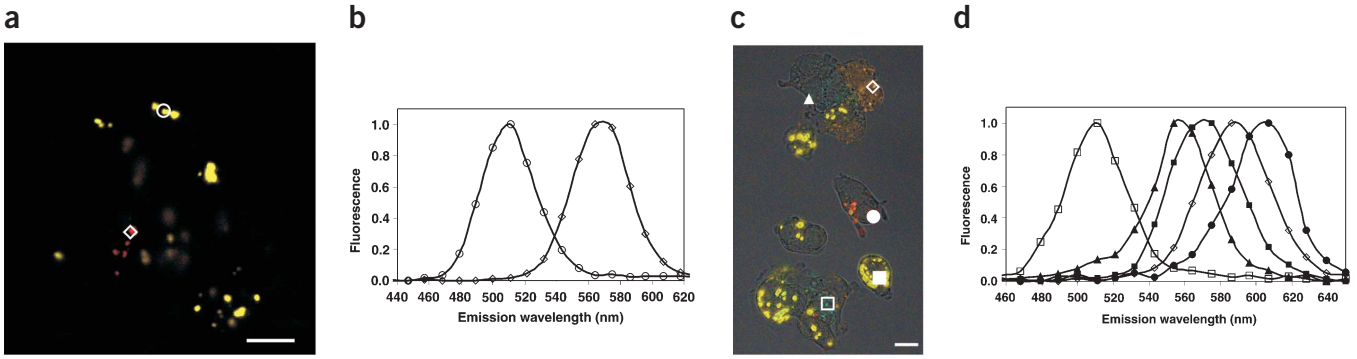

Figure 5 Emission-scanning multiphoton microscopy can identify at least five populations of cells. (**a**) B16F10 cells were labeled with different QDs and the cells were combined and injected in the tail vein of mice. After 5 h lung tissues were prepared as in **Figure 1d** and cells were imaged with emission-scanning multiphoton microscopy in lung tissues (excitation of 820 nm). (**b**) The regions used for the emission scans are depicted in the multiphoton images (circles, 510-nm QDs; diamonds, 570-nm QDs). (**c**) B16F10 cells were labeled with five different QDs (510 nm, 550 nm, 570 nm, 590 nm and 610 nm) and they were combined, plated on a coverslip and then imaged with emission-scanning multiphoton microscopy (excitation of 820 nm). (**d**) Emission scans used a 10-nm bandwidth. Each color QD is represented by a different symbol in the graph. The symbol on the multiphoton image matches the profile seen on the graph. Scale bars, 10 μm. Fluorescence measurements are given in arbitrary units.

multiphoton emission-scanning microscopy to simultaneously image different QD-labeled tumor cells in tissues. Illuminating with the 820-nm tuned pulsed laser, cells labeled with the 510-nm and 570-nm QDs were efficiently identified in tissues (**Fig. 5a**,**b**). To test the usefulness of combining multiphoton excitation and the use of multiple QDs, we mixed together five groups of B16F10 cells, each labeled with QDs emitting a different color of QD (510 nm, 550 nm, 570 nm, 590 nm and 610 nm). Using emission-scanning multiphoton microscopy, we were able to identify each of the five populations of cells (**Fig. 5c**,**d**). If, instead of using single-color QDs, cells are tagged using a combination of different QDs, then the ability to resolve five colors would provide 36 unique tags, which permits simultaneously resolving 36 different populations of cells.

DISCUSSION

Our results indicate that QDs are inert fluorescent tags suitable for labeling cells for *in vivo* studies. QD labeling has no detectable toxicity to the labeled cells or the host animal. The emission properties of QDs provide a means to overcome the difficulty of tissue autofluorescence, to which other fluorescent tags, such as green fluorescent protein, are still subject. Thus, fluorescence can be used to study single cells at early stages of metastasis and examine this process at the single-cell level in a natural tissue environment. The use of QDs in conjunction with multiphoton and emission-scanning microscopy provides the opportunity to simultaneously identify and study the interactions of multiple different populations of tumor cells and tissue cells within the same animal. Development of these tools opens up the potential not only to study tumor cell extravasation and invasion into tissues in real time, but also to test models pertaining to interactions between different tumor cells and their interactions with the host cells. These tools may also permit studying a variety of other multicellular interactions that occur during growth and development of animals.

METHODS

Cell culture. B16F10 melanoma cells (ATCC CRL-6475, American Type Culture Collection) were cultured at 37 °C in a humidified atmosphere containing 5% CO_2 with Dulbecco's modified Eagle medium (11965-092 Gibco-Invitrogen) supplemented with 10% fetal bovine serum.

QD loading. The QDs used here are DHLA-capped and made in-house as described[16]. The synthesis of water-soluble CdSe-ZnS nanoparticles involved growth of core nanocrystal using organometallic precursors. The core was overcoated with ZnS, capped with TOP/TOPO and precipitated in a size-selective manner. The DHLA-cap exchange was carried out, and the QDs were washed to remove excess free cap. The aqueous suspensions of QDs of indicated emission wavelength and concentration were stored for future use. Two days before loading, we plated 5×10^4 B16F10 cells in each well of a 6-well tissue culture plate containing 2 ml of medium. The cells were loaded using Lipofectamine 2000 (Invitrogen). The mixture contained 100 μl of Opti-MEM (11058-021, Gibco-Invitrogen), 4 μl of Lipofectamine 2000 and 10 μl of QDs (with a final concentration as a low as 10 pmol). B16F10 cells were incubated in the loading mixture for 4–6 h. Cell culture medium was then used to rinse the cells three times. The cells were then left overnight in fresh medium. For labeling cells with cell tracker dyes (Molecular Probes), 10 μM orange cell tracker CMTMR (C-2927) or blue cell tracker (4-chloromethyl-7-hydroxycoumarin, C-2111) was incubated with B16F10 cells in culture medium for 1 h in a cell culture incubator. The cells were then washed three times in excess phosphate-buffered saline (PBS) before use.

Tail-vein injection. All experimental protocols met the approval of the Rockefeller University Laboratory Animal Research Center (LARC protocol 02106). Before injection, B16F10 cells were treated with trypsin and washed three times using fresh cell culture medium. The cells were suspended in a 1:5 mixture of serum-free Dulbecco's modified Eagle medium and PBS such that 100 μl contained either 2×10^5 or 4×10^5 cells. In all, 2×10^5 cells were put back into culture for assessing the QD labeling efficiency. These counts were accomplished by searching random fields of ten sets of ten isolated cells using a Nikon Diaphot fluorescence microscope equipped with sliding emission filters and a ×40 (Ph3 DL, NA 0.55) air lens, and scoring for the presence or absence of QDs. For each experiment a maximum of 100 μl of cells were injected into the tail vein of age- and sex-matched C57BL/6 mice (The Jackson Laboratory). Depending on the experiment, mice were killed by means of CO_2 asphyxiation between 1 and 6 h later.

Tissue preparation. Tissues were removed and either diced for whole mounts and then fixed in 10% phosphate-buffered formalin or fixed intact and then whole-mounted. The tissues remained in the fixative overnight and then were washed in three rinses of PBS the following day. Histological sections (5–10 μm thick) were prepared by T. Rosati (Histo-Path Services). Some tissues were stained with actin (1:10 (v/v) Alexa Fluor 633 phalloidin, Molecular Probes) for 1 h or fluorescein lycopersicon esculentum lectin (500 mg ml^{-1}, Vector Laboratories) and then whole-mounted on slides using Glycergel (Dako). Other tissues were simply whole-mounted without staining.

One- and two-photon microscopy. Tissues were analyzed and images collected using a Zeiss LSM 510 META one- or two-photon microscope (titanium sapphire femtosecond laser, Coherent). A ×63 (Plan-Apochromat, NA 1.40) water immersion objective was used for histological sections, whereas a ×63 (IR-Achroplan, NA 0.90) dipping lens was used for tissue whole mounts. For emission-scanning microscopy, fluorescence emission from each pixel in the image plane was captured at 10-nm wavelength intervals using the Zeiss META detector and a full spectral scan. Settings for the META detector for individual images are included in the figure legends. One-photon META counts were conducted on lung tissue whole mounts as follows: for injections of single populations of QD-labeled B16F10 cells, ten sets of ten cells were scored for the presence of QDs, using a ×63 (IR-Achroplan, NA 0.90) dipping lens; for experiments in which two populations of QD-labeled cells were injected, the number of cells loaded with each color QD were scored for 50 fields from lung tissues using a ×20 (Plan-Apochromat, NA 0.75) air lens.

Note: Supplementary information is available on the Nature Medicine website.

ACKNOWLEDGMENTS

This work was supported by the Cancer Research Institute (E.B.V.), the American Cancer Society (RPG-98-177-01-CDD, S.M.S.) and the National Science Foundation (NSF BES-0119468, S.M.S.). H.M. acknowledges K. Ward and A. Ervin at the Office of the Naval Research for research support (ONR N001400WX20094). The views, opinions and findings described in this report are those of the authors and should not be construed as official Department of the Navy positions, policies or decisions. The authors wish to thank A. North and the Bio-Imaging Resource Center of Rockefeller University and B. Sanchez from the Rockefeller University Laboratory Animal Resource Center, for excellent support.

COMPETING INTERESTS STATEMENT

The authors declare that they have no competing financial interests.

Received 22 January; accepted 28 June 2004
Published online at http://www.nature.com/naturemedicine/

1. Chambers, A.F., Groom, A.C. & MacDonald, I.C. Dissemination and growth of cancer cells in metastatic sites. *Nat. Rev. Cancer* **2**, 563–572 (2002).
2. Fidler, I.J. The pathogenesis of cancer metastasis: the 'seed and soil' hypothesis revisited. *Nat. Rev. Cancer* **3**, 453–458 (2003).
3. Friedl, P. & Wolf, K. Tumour-cell invasion and migration: diversity and escape mechanisms. *Nat. Rev. Cancer* **3**, 362–374 (2003).
4. Lewalle, J.M. *et al.* Alteration of interendothelial adherens junctions following tumor cell-endothelial cell interaction *in vitro*. *Exp. Cell Res.* **237**, 347–356 (1997).
5. Voura, E.B., Chen, N. & Siu, C.H. Platelet-endothelial cell adhesion molecule-1 (CD31) redistributes from the endothelial junction and is not required for the transendothelial migration of melanoma cells. *Clin. Exp. Metastasis* **18**, 527–532 (2000).
6. Voura, E.B., Ramjeesingh, R.A., Montgomery, A.M., & Siu, C.H. Involvement of integrin a(v)b(3) and cell adhesion molecule L1 in transendothelial migration of melanoma cells. *Mol. Biol. Cell* **12**, 2699–2710 (2001).
7. Lim, D.S. *et al.* Antitumor efficacy of reticulol from Streptoverticillium against the lung metastasis model B16F10 melanoma. Lung metastasis inhibition by growth inhibition of melanoma. *Chemotherapy* **49**, 146–153 (2003).
8. Yamaguchi, H. *et al.* Sphingosine-1-phosphate receptor subtype-specific positive and negative regulation of Rac and haematogenous metastasis of melanoma cells. *Biochem. J.* **374**, 715–722 (2003).
9. Dove, A. MMP inhibitors: glimmers of hope amidst clinical failures. *Nat. Med.* **8**, 95 (2002).
10. Al Mehdi, A.B. *et al.* Intravascular origin of metastasis from the proliferation of endothelium-attached tumor cells: a new model for metastasis. *Nat. Med.* **6**, 100–102 (2000).
11. Naumov, G.N. *et al.* Persistence of solitary mammary carcinoma cells in a secondary site: a possible contributor to dormancy. *Cancer Res.* **62**, 2162–2168 (2002).
12. Brown, E.B. *et al.* *In vivo* measurement of gene expression, angiogenesis and physiological function in tumors using multiphoton laser scanning microscopy. *Nat. Med.* **7**, 864–868 (2001).
13. Wang, W. *et al.* Single cell behavior in metastatic primary mammary tumors correlated with gene expression patterns revealed by molecular profiling. *Cancer Res.* **62**, 6278–6288 (2002).
14. Zhang, J., Campbell, R.E., Ting, A.Y. & Tsien, R.Y. Creating new fluorescent probes for cell biology. *Nat. Rev. Mol. Cell Biol.* **3**, 906–918 (2002).
15. Jaiswal, J.K. & Simon, S.M. Potentials and pitfalls of fluorescent quantum dots for biological imaging. *Trends Cell Biol.* in the press.
16. Mattoussi, H. *et al.* Self-assembly of CdSe-ZnS quantum dot bioconjugates using an engineered recombinant protein. *J. Am. Chem. Soc.* **122**, 12142–12150 (2000).
17. Wu, X. *et al.* Immunofluorescent labeling of cancer marker Her2 and other cellular targets with semiconductor quantum dots. *Nat. Biotechnol.* **21**, 41–46 (2003).
18. Larson, D.R. *et al.* Water-soluble quantum dots for multiphoton fluorescence imaging in vivo. *Science* **300**, 1434–1436 (2003).
19. Chan, W.C. *et al.* Luminescent quantum dots for multiplexed biological detection and imaging. *Curr. Opin. Biotechnol.* **13**, 40–46 (2002).
20. Dabbousi, B.O. *et al.* (CdSe)ZnS core-shell quantum dots: synthesis and characterization of a size series of highly luminescent nanocrystallites. *J. Phys. Chem.* **101**, 9463–9475 (1997).
21. Lim, Y.T. *et al.* Selection of quantum dot wavelengths for biomedical assays and imaging. *Mol. Imaging* **2**, 50–64 (2003).
22. Mattoussi, H., Kuno, M.K., Goldman, E.R., George, P. & Mauro, J.M. in *Optical Biosensors: Present and Future*. (eds. F.S. Ligler & C.A. Rowe) 537–569 (Elsevier, The Netherlands, 2002).
23. Jaiswal, J.K., Mattoussi, H., Mauro, J.M. & Simon, S.M. Long-term multiple color imaging of live cells using quantum dot bioconjugates. *Nat. Biotechnol.* **21**, 47–51 (2003).
24. Fidler, I.J. Biological behavior of malignant melanoma cells correlated to their survival *in vivo*. *Cancer Res.* **35**, 218–224 (1975).
25. Fidler, I.J., Pollack, V.A. & Hanna, N. The use of nude mice for studies of cancer metastasis in immune-deficient animals. in *4th International Workshop on Immune-Deficient Animals in Experimental Research* 328–338 (Karger, New York, 1984).
26. Zuhorn, I.S. & Hoekstra, D. On the mechanism of cationic amphiphile-mediated transfection. To fuse or not to fuse: is that the question? *J. Membr. Biol.* **189**, 167–179 (2002).
27. Clark, P.R. & Hersh, E.M. Cationic lipid-mediated gene transfer: current concepts. *Curr. Opin. Mol. Ther.* **1**, 158–176 (1999).
28. Dickinson, M.E., Simbuerger, E., Zimmermann, B., Waters, C.W. & Fraser, S.E. Multiphoton excitation spectra in biological samples. *J. Biomed. Opt.* **8**, 329–338 (2003).
29. Ballou, B., Lagerholm, B.C., Ernst, L.A., Bruchez, M.P. & Waggoner, A.S. Noninvasive imaging of quantum dots in mice. *Bioconjug. Chem.* **15**, 79–86 (2004).
30. Derfus, A.M., Chan, W.C.W. & Bhatia, S.N. Probing the cytotoxicity of semiconductor quantum dots. *Nano Letters* **4**, 11–18 (2004).